Photocatalytic Conversion of Carbon Dioxide Using Zn–Cu–Ga Layered Double Hydroxides Assembled with Cu Phthalocyanine: Cu in Contact with Gaseous Reactant is Needed for Methanol Generation

Shogo Kawamura, Naveed Ahmed, Gabriela Carja, Yasuo Izumi

Dossier

This paper is a part of the hereunder thematic dossier published in OGST Journal, Vol. 70, No. 5, pp. 791-902 and available online here

Cet article fait partie du dossier thématique ci-dessous publié dans la revue OGST, Vol. 70, n°5, pp. 791-902 et téléchargeable ici

DOSSIER Edited by/Sous la direction de : **D. Uzio**

IFP Energies nouvelles International Conference / Les Rencontres Scientifiques d'IFP Energies nouvelles

PHOTO4E – Photocatalysis for energy

PHOTO4E – Photocatalyse pour l'énergie

Oil & Gas Science and Technology – Rev. IFP Energies nouvelles, Vol. 70 (2015), No. 5, pp. 791-902

IFP Energies nouvelles

Oil & Gas Science and Technology – Rev. IFP Energies nouvelles, Vol. 70 (2015), No. 5, pp. 841-852

DOI: 10.2516/ogst/2015020

IFP Energies nouvelles International Conference
Rencontres Scientifiques d'IFP Energies nouvelles

PHOTO4E – Photocatalysis for energy
PHOTO4E – Photocatalyse pour l'énergie

Photocatalytic Conversion of Carbon Dioxide Using Zn–Cu–Ga Layered Double Hydroxides Assembled with Cu Phthalocyanine: Cu in Contact with Gaseous Reactant is Needed for Methanol Generation

Shogo Kawamura[1], Naveed Ahmed[1], Gabriela Carja[2] and Yasuo Izumi[1]*

[1] *Department of Chemistry, Graduate School of Science, Chiba University, Yayoi 1-33, Inage-ku, Chiba 263-8522 - Japan*
[2] *Department of Chemical Engineering, Faculty of Chemical Engineering and Environmental Protection, Technical University "Gh. Asachi" of Iasi, Bd. Mangeron No. 71, Iasi 700554 - Romania*
e-mail: x0s3033@students.chiba-u.jp - nedoanjum@yahoo.com - carja@uaic.ro - yizumi@faculty.chiba-u.jp

* Corresponding author

Abstract *— Photocatalytic conversion of CO_2 into fuels is an attractive option in terms of both reducing the increased concentration of atmospheric CO_2 as well as generating renewable hydrocarbon fuels. It is necessary to investigate good catalysts for CO_2 conversion and to clarify the mechanism irradiated by natural light. Layered Double Hydroxides (LDH) have been attracting attention for CO_2 photoreduction with the expectation of sorption capacity for CO_2 in the layered space and tunable semiconductor properties as a result of the choice of metal cations. This study first clarifies the effects of Cu doping to LDH comprising Zn and Al or Ga. Cu could be incorporated in the cationic layers of LDH as divalent metal cations and/or interlayer anions as $Cu(OH)_4^{2-}$. The formation rates of methanol and CO were optimized for $[Zn_{1.5}Cu_{1.5}Ga(OH)_8]^+{}_2Cu(OH)_4^{2-}{\cdot}mH_2O$ at a total rate of 560 nmol h^{-1} $g_{cat}{}^{-1}$ irradiated by UV–visible light. Cu phthalocyanine tetrasulfonate hydrate ($CuPcTs^{4-}$) and silver were effective as promoters of LDH for CO_2 photoreduction. Especially, the total formation rate using CuPcTs-$[Zn_3Ga(OH)_8]^+{}_2CO_3^{2-}{\cdot}mH_2O$ irradiated by visible light was 73% of that irradiated by UV–visible light. The promotion was based on HOMO–LUMO excitation of $CuPcTs^{4-}$ by visible light. The LUMO was distributed on N atoms of pyrrole rings bound to central Cu^{2+} ions. The photogenerated electrons diffused to the Cu site would photoreduce CO_2 progressively in a similar way to inlayer and interlayer Cu sites in the LDH in this study.*

Résumé — Conversion photocatalytique du dioxyde de carbone par des hydroxydes doubles lamellaires de Zn–Cu–Ga promus par la phtalocyanine de Cu : nécessité du contact entre le Cu et le réactif gazeux pour la synthèse du méthanol — La conversion photocatalytique de CO_2 est une option attractive pour limiter la concentration du CO_2 atmosphérique quand elle a pour objectif la production de produits hydrocarbonés utilisés comme carburants renouvelables. Néanmoins, des études sont encore nécessaires pour étudier les catalyseurs de conversion de CO_2 et clarifier les mécanismes réactionnels. Des Hydroxydes Doubles Lamellaires (HDL) sont des catalyseurs intéressants pour la photoréduction de CO_2 et l'on s'attend à obtenir une capacité d'adsorption du

CO_2 dans l'espace interlamellaire et des propriétés semi-conductrices adaptables par le choix des cations métalliques. La présente étude démontre tout d'abord les effets du dopage du Cu dans les HDL comprenant du Zn et de l'Al ou du Ga. Le cuivre pourrait être incorporé dans les couches cationiques des HDL sous forme de cations métalliques divalents et/ou d'anions inter-feuillets sous forme de $Cu(OH)_4^{2-}$. Les taux de formation du méthanol et du CO ont été optimum pour le $[Zn_{1.5}Cu_{1.5}Ga(OH)_8]^+{}_2Cu(OH)_4^{2-}{\cdot}mH_2O$ correspondant à une vitesse totale de 560 nmol h^{-1} $g_{cat}{}^{-1}$, sous irradiation UV visible. Le tétrasulfonate-hydrate de phtalocyanine de Cu ($CuPcTs^{4-}$) et l'argent se sont avérés être des promoteurs efficaces de HDL pour la photoréduction du CO_2. En particulier, le taux de formation total en utilisant du CuPcTs-$[Zn_3Ga(OH)_8]^+{}_2CO_3^{2-}{\cdot}mH_2O$ irradié par la lumière visible représentait 73% de celui irradié par de la lumière UV visible. La promotion a été attribuée à une excitation HOMO–LUMO du $CuPcTs^{4-}$ par la lumière visible. Le LUMO répartie sur l'atome d'azote des cycles des pyrroles lié à l'ion central Cu^{2+}. Les électrons photogénérés diffusés sur le site de Cu photoréduiraient le CO_2 sur les sites cationiques (dans les couches) ou anioniques (interfeuillets) des HDL.

INTRODUCTION

Photocatalytic conversion of CO_2 into fuels has emerged as an attractive option, in terms of both reducing the increased concentration of atmospheric CO_2 as well as generating renewable hydrocarbon fuels that can be directly supplied to our present energy infrastructure (Costentin *et al.*, 2013; Corma and García, 2013; Genevese *et al.*, 2013; Habisreutinger *et al.*, 2013; Indrakanti *et al.*, 2009; Izumi, 2013; Kubacka *et al.*, 2012; Lewis and Nocera, 2006; Lv *et al.*, 2012; Roy *et al.*, 2010). The photocatalytic conversion of CO_2 involves two reaction steps:

$$2H_2O(g) \rightarrow 2H_2(g) + O_2(g), \qquad \Delta G_r^{\circ} = 689\,\text{kJ mol}^{-1} \quad (1)$$

$$CO_2(g) + 3H_2(g) \rightarrow CH_3OH(g) + H_2O(g), \qquad \Delta G_r^{\circ} = 2.9\,\text{kJ mol}^{-1} \quad (2)$$

It is important to investigate good catalysts for CO_2 conversion into fuels using hydrogen as a reductant (Eq. 2), which is potentially obtained from photocatalytic water splitting (Eq. 1) (Izumi, 2013; Ahmed *et al.*, 2011).

In this study, catalysts for converting CO_2 into methanol using hydrogen and UV–visible light were investigated. Layered Double Hydroxides (LDH) $[M^{II}{}_{1-x}M^{III}{}_x(OH)_2]^{x+}X^{2-}{}_{x/2}{\cdot}mH_2O$ (M^{II} = Zn, Cu; M^{III} = Al, Ga; X = CO_3, $Cu(OH)_4$; m~1/2) were chosen with the expectation of:

- sorption capacity for CO_2 in the layered space,
- tunable semiconductor properties as a result of the choice of metal cations

(Ahmed *et al.*, 2013; Cavani *et al.*, 1991; Fan *et al.*, 2014; Li *et al.*, 2014; Sideris *et al.*, 2008; Zümreoglu-Karan and Ay, 2012).

Furthermore, to utilize visible light as the major part of the solar spectrum, dyes/nanoparticles were mixed with the LDH. Especially, the effects of Cu phthalocyanine tetrasulfonate hydrate ($CuPcTs^{4-}$) combined with LDH were studied.

1 EXPERIMENTAL SECTION

A LDH compound of $[Zn_3Ga(OH)_8]^+{}_2CO_3^{2-}{\cdot}mH_2O$ was synthesized using a reported procedure from metal nitrates, Na_2CO_3, and NaOH controlled at pH 8 (Ahmed *et al.*, 2011). This compound is abbreviated as $Zn_3Ga|CO_3$. Similarly, LDH comprising various compositions of $[M^{II}{}_3M^{III}(OH)_8]^+{}_2X^{2-}{\cdot}mH_2O$ (X = CO_3, $Cu(OH)_4$) were synthesized from nitrates of Zn, Cu, Al and Ga, and sodium carbonate/ammonium tetrachlorocuprate dihydrate at pH 8 (Ahmed *et al.*, 2012). The formula is abbreviated as $M^{II}{}_3M^{III}|X$.

$Na^+{}_4CuPcTs^{4-}$ was purchased from *Aldrich* (purity >85%) and used without further purification. For the ion exchange method, we followed the procedure presented in reference (Parida *et al.*, 2007). Firstly, 0.50 g of $Zn_3Ga|CO_3$ powder was immersed in an aqueous solution of $Na^+{}_4CuPcTs^{4-}$ (0.60 mM, 25 mL) in a flask and magnetically stirred at 900 rotations per minute (rpm) for 24 h. The blue precipitates that were obtained were filtered using a polytetrafluoroethylene-based membrane filter (Omnipore JGWP04700, *Millipore*) with a pore size of 0.2 µm and washed well with deionized water (<0.06 µS cm^{-1}; total 250 mL). The precipitates that were obtained were dried under vacuum at 290 K for 24 h. The blue sample was denoted as CuPcTs-$Zn_3Ga|CO_3$. The loading of Cu was 0.19 wt%.

Anion exchange of $Zn_3Ga|NO_3$ with $Na^+{}_4CuPcTs^{4-}$ was performed following the procedure in the literature (Abellán *et al.*, 2012). All of the procedure until the drying under vacuum was conducted under an argon atmosphere. 0.30 g of $Zn_3Ga|NO_3$ powder was placed in a flask and an aqueous solution of $Na^+{}_4CuPcTs^{4-}$ (5.0 mM, 200 mL) was slowly added and magnetically stirred at 900 rpm. Then, 30 mL of ethylene glycol and 30 mL of ethanol were added to the flask. The mixture was agitated by ultrasound (430 W, 38 kHz) for 10 min and then was magnetically stirred at 900 rpm for 3 days.

The precipitates that were obtained were filtered using an Omnipore JGWP04700 filter and washed well with ethanol (total 250 mL) and deionized water (total 250 mL). The precipitates that were obtained were dried at 290 K for 24 h under vacuum. The sample was denoted as $Zn_3Ga|CuPcTs$.

Ag nitrate was impregnated from aqueous solution with $Zn_3Ga|CO_3$. The loading of Ag was 0.36 wt% (Kawamura *et al.*, 2015). The sample was denoted as Ag-$Zn_3Ga|CO_3$. Separately, the assembly of Au nanoparticles with $Zn_3Ga|CO_3$ was obtained using the structural reconstruction of LDH in the aqueous solutions containing Au^{3+} (Carja *et al.*, 2013). Hence, 1.20 g $Zn_3Ga|CO_3$ powder was calcined in an oven at 773 K for 8 h. Freshly calcined $Zn_3Ga|CO_3$ powder was directly added to 200 mL aqueous solution of Au(III) acetate (>99.9%, *Alfa Aesar*; 0.10 g) stirring at a rate of 900 rpm. The pH of the solution was adjusted to 8.0 by the addition of NaOH aqueous solution (0.10 M). The reaction mixture was stirred at the rate of 900 rpm and 290 K for 20 min and at the rate of 150 rpm and 313 K for 5 h. Then, the precipitate was centrifuged at the rate of 10 000 rpm and dried in an oven at 353 K for 1 h. The color of the catalyst obtained was light purple. The sample was denoted as Au-$Zn_3Ga|CO_3$.

Optical spectroscopic measurements were performed using a UV–visible spectrophotometer (model V-650, *JASCO*) using D_2 and halogen lamps for wavelengths between 200 and 340 nm and 340 and 800 nm, respectively. An integrating sphere (model ISV-469, *JASCO*) was used for the Diffuse Reflectance (DR) measurements. The samples were set in contact with the quartz window glass in gas-tight DR cells. Measurements were performed at 290 K within the wavelength range 200-800 nm using 70 mg of sample. DR spectra were converted to absorption spectra on the basis of the Kubelka–Munk equation (Ahmed *et al.*, 2011, 2012). The band-gap (E_g) value was evaluated on the basis of either simple extrapolation of the absorption edge or the fit to the Davis–Mott equation:

$$\alpha \times h\nu \propto \left(h\nu - E_g\right)^n \tag{3}$$

in which α, h, and ν are the absorption coefficient, Planck's constant and the frequency of light, respectively, and n is 1/2, 3/2, 2 and 3 for allowed direct, forbidden direct, allowed indirect and forbidden indirect electronic transitions, respectively (Wooten, 1972).

The Brunauer-Emmett-Teller surface area (S_{BET}) was calculated on the basis of eight-point measurements between 10 and 46 kPa in the N_2 adsorption isotherm at 77 K. The X-Ray Diffraction (XRD) pattern was observed using a D8 ADVANCE diffractometer (*Bruker*) at the Center for Analytical Instrumentation, Chiba University, at a Bragg angle of $2\theta_B = 3\text{-}60°$ with a scan step of 0.01° and a scan rate of 5 s per step. The measurements were performed at 40 kV and 40 mA using Cu Kα emission and a nickel filter.

Cu K-edge X-ray Absorption Fine Structure (XAFS) spectra were measured at 290 K in transmission mode in the Photon Factory Advanced Ring at the High Energy Accelerator Research Organization (*Tsukuba*) on beamline NW10A. The storage ring energy was 6.5 GeV and the ring current was 46.6-36.1 mA. A Si (311) double-crystal monochromator and platinum-coated focusing cylindrical mirror were inserted into the X-ray beam path. The X-ray intensity was maintained at 65% of the maximum flux using a piezo translator set to the crystal. The slit opening size was 1 mm (vertical) × 2 mm (horizontal) in front of the ionization chamber. Part of the XAFS measurements were performed for a sample in a reactor equipped with polyethylene naphthalate windows (Q51-16, *Teijin*) irradiated by a xenon arc lamp (Morikawa *et al.*, 2014a; Izumi *et al.*, 2007). The Cu K-edge absorption energy was calibrated to 8 980.3 eV for the spectrum of Cu metal foil (Bearden, 1967).

The XAFS data were analyzed using an XDAP (X-ray absorption fine structure Data Analysis Program) package (Vaarkamp *et al.*, 2006). The pre-edge background was approximated by a modified Victoreen function $C_2/E^2 + C_1/E + C_0$. The background of the post-edge oscillation was approximated by a smoothing spline function and calculated by an equation for the number of data points, where k is the wavenumber of photoelectrons:

$$\sum_{i=1}^{\text{Data Points}} \frac{(\mu x_i - BG_i)^2}{\exp\left(-0.075k_i^2\right)} \leq \text{smoothing factor} \tag{4}$$

Multiple-shell curve-fit analyses were performed for the Fourier-filtered k^3-weighted Extended X-ray Absorption Fine Structure (EXAFS) data in k- and R-space using empirical amplitude extracted from the EXAFS data for $Na^+{}_4CuPcTs^{4-}$ (Izumi *et al.*, 2005, 2009). The interatomic distance (R) and its associated coordination number (N) for the Cu–N pair were set to 0.1950 nm with a N value of 4 (Carrera *et al.*, 2004). The many-body reduction factor $S_0{}^2$ was assumed to be equal for both the sample and the reference.

As-synthesized and preheated samples of the LDH CuPcTs-$Zn_3Ga|CO_3$, Ag-$Zn_3Ga|CO_3$ and Au-$Zn_3Ga|CO_3$

were tested for the photocatalytic conversion of CO_2 (Kawamura *et al.*, 2015). The tests were conducted in a closed circulating system (171 mL) equipped with a photoreaction quartz cell that had a flat bottom (23.8 cm^2). 100 mg of the LDH catalyst was uniformly spread in the photoreaction cell and was evacuated by rotary and diffusion pumps (10^{-6} Pa) at 290 K for 2 h until the desorbed gas was detected by an online Gas Chromatograph (GC). 2.3 kPa of CO_2 (0.177 mmol) and 21.7 kPa of H_2 (1.67 mmol) were introduced to both intact and pretreated LDH photocatalysts and were allowed to circulate for 30 min in contact with the catalyst to attain sorption equilibrium before irradiation.

The photocatalyst was then irradiated with UV–visible light from the 500-W xenon arc lamp (*Ushio*, model UI-502Q) upward through the flat bottom of the quartz reactor for 5 h. The distance between the bottom of the reactor and the lamp house exit window was set to 20 mm. The light intensity was 42 mW cm^{-2} at the center of the sample cell and 28 mW cm^{-2} at the periphery of the bottom plate of the sample cell. The temperature was within the range 305-313 K at the catalyst position during the illumination for 5 h. As a comparison, the photocatalyst was irradiated with visible light using one of the following UV-cut filters between the light exit of UI-502Q and the photocatalyst. Photocatalytic CO_2 reduction tests were performed systematically using L42, Y52, O58, R62, R66 and W-R715 sharp cut filters (*Hoya*) between the irradiation light exit and photoreactor. The thickness was 2.5 mm except for W-R715 (2.0 mm). These filters pass the light of wavelengths greater than 420, 520, 580, 620, 660 and 715 nm, respectively. The transmittance of nonfiltered light was more than 88% for L42, Y52, O58, R62 and R66, and almost 100% for W-R715 (manufacturer's web information[(1)]). Products and reactants were analyzed using packed columns of a 13X-S molecular sieve and PolyEthylene Glycol (PEG-6000) supported on Flusin P (*GL Sciences*) set in the online GC equipped with a thermal conductivity detector (*Shimadzu*, model GC-8A).

The molecular orbitals for $CuPcTs^{4-}$ were calculated using Gaussian 09 (*Gaussian, Inc.*, Wallingford, Connecticut, USA) employing a polarized basis set of 6-31G(d) and in density functional theory mode to calculate the electron correlation using the functional B3LYP (Rauf *et al.*, 2012).

2 RESULTS

2.1 Characterization

The interlayer interval and S_{BET} of the LDH synthesized were between 0.751-0.792 nm and 35-70 m^2 g^{-1}, respectively, except for $Zn_3Ga|CuPcTs$. The metal cations existed in nearly identical octahedral MO_6 coordination environments in cationic sheets based on the similarity of the Zn K, Cu K and Ga K-edge X-ray Absorption Near-Edge Structure (XANES) (Ahmed *et al.*, 2011, 2012).

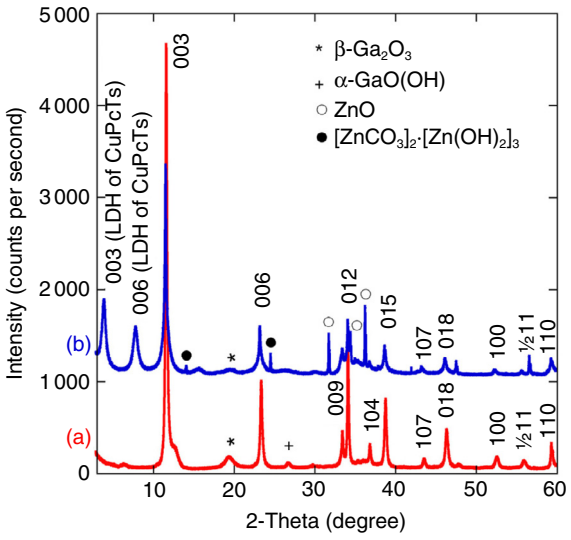

Figure 1

XRD patterns for a) CuPcTs-$Zn_3Ga|CO_3$ and b) $Zn_3Ga|CuPcTs$.

The layered structure of the LDH synthesized in this study was confirmed by XRD. The XRD pattern for CuPcTs-$Zn_3Ga|CO_3$ is depicted in Figure 1a. The diffraction peaks at $2\theta_B$ = 11.7°, 23.4°, 33.5°, 34.2°, 36.9°, 38.8°, 43.6°, 46.4°, 52.6°, 56.9° and 59.4° were assigned to (003), (006), (009), (012), (104), (015), (107), (018), (100), ($\frac{1}{2}$11) [=(01$\bar{1}$1)] and (110) diffraction, respectively, for the regular layered structure of the LDH. The interlayer interval value was evaluated at 0.755 nm on the basis of the (003) diffraction angle and changed negligibly as compared with $Zn_3Ga|CO_3$ (0.751 nm; Ahmed *et al.*, 2011).

The pattern is compared with that for $Zn_3Ga|CuPcTs$ (Fig. 1b-line). Two peaks at $2\theta_B$ = 4.04° and 7.91° appeared assignable to (003) and (006) diffraction of the LDH with the interlayer anions of $CuPcTs^{4-}$ (Abellán *et al.*, 2012). The interlayer interval value was evaluated at 2.18 nm on the basis of the (003) diffraction angle due to the intercalation of larger $CuPcTs^{4-}$ anions. The diffraction peaks at $2\theta_B$ = 11.6°, 23.3°, 33.5°, 34.2°, 36.3°, 38.7°, 43.2°, 46.2°, 52.3°, 56.6° and 59.3° also appeared, and suggested the by-product phase of $Zn_3Ga|CO_3$. The interlayer interval value was evaluated at 0.760 nm on the basis of the (003) diffraction angle for the by-product phase.

In the pattern for both samples, a very small amount of impurity peaks was observed at 19.5-19.6° and 26.8° owing

[1] *Hoya*, web information of sharp cut filters: http://www.hoyaoptics.com/color_filter/sharp_cut.htm, http://buyersguide.pennwell.com/Shared/User/pr9f6c58fbba904eefa88c895cd0f5f336.pdf.

TABLE 1

The band-gap values and the type of electronic transition based on UV–visible spectra for Zn-Cu-Ga LDH

Photocatalyst	Band gap (eV)	e^- transition
$Zn_3Ga\|CO_3$	5.6	Direct
$Zn_{1.5}Cu_{1.5}Ga\|CO_3$	3.5	Forbidden direct
$Zn_3Al\|CO_3$	5.7	Direct
$Zn_{1.5}Cu_{1.5}Al\|CO_3$	4.1	Direct
$Zn_3Ga\|Cu(OH)_4$	4.2 (impurity phase: 3.2)	Direct
$Zn_{1.5}Cu_{1.5}Ga\|Cu(OH)_4$	3.0	Direct

to β-Ga_2O_3 and α-GaO(OH), respectively (Fig. 1). In the pattern for $Zn_3Ga|CuPcTs$, a small amount of impurity peaks at 31.9°, 34.5° and 36.3° owing to ZnO and those at 14.2° and 24.6° owing to $[ZnCO_3]_2{\cdot}[Zn(OH)_2]_3$ also appeared (b-line).

The E_g values were evaluated by the extrapolation of the absorption edge in the UV–visible spectra. The values given were within the range 5.6-3.0 eV for $Zn_3Ga|CO_3$, $Zn_{1.5}Cu_{1.5}Ga|CO_3$, $Zn_3Al|CO_3$, $Zn_{1.5}Cu_{1.5}Al|CO_3$, $Zn_3Ga|Cu(OH)_4$ and $Zn_{1.5}Cu_{1.5}Ga|Cu(OH)_4$ (Tab. 1).

Besides the absorption edge for the LDH, an intense absorption peak appeared at 678 nm for CuPcTs-$Zn_3Ga|CO_3$ (Fig. 2b-line, solid line). The UV–visible spectrum for CuPcTs-$Zn_3Ga|CO_3$ basically resembled that for aqueous solution of $Na^+_4CuPcTs^{4-}$ (Fig. 2a-line); however, the peak intensity ratio in the range 600-700 nm was different: 678 nm (s), 630 nm (sh) and 612 nm (sh) for CuPcTs-$Zn_3Ga|CO_3$ *versus* 630 nm (s) and 660 nm (sh) for aqueous solution of $Na^+_4CuPcTs^{4-}$. As the peaks at 678-660 nm or 630 nm would be assigned to HOMO (a_{1u})–LUMO (e_g) electronic transition (Q-band, Fig. 3), the HOMO and/or LUMO of $CuPcTs^{4-}$ were significantly perturbed by the interaction with the $Zn_3Ga|CO_3$ surface.

As compared with the Q-band, the peaks at 337-340 nm were assigned to transition from a_{2u} to LUMO (e_g) (Soret band). The peak at 220 nm was only observed for aqueous solution of $Na^+_4CuPcTs^{4-}$ (Fig. 2a-line). This peak would be a transition from a slightly deeper level than a_{2u} to LUMO (e_g) or from a_{2u} to a slightly shallower level than LUMO (e_g) (Marom *et al.*, 2008).

The UV–visible spectrum for CuPcTs-$Zn_3Ga|CO_3$ used for photocatalytic tests under $CO_2 + H_2$ for 5 h was also measured (Fig. 2b-line, dotted line). The spectrum was essentially identical to that for the fresh sample (solid line), indicating the stability of $CuPcTs^{4-}$ dispersed over $Zn_3Ga|CO_3$ under the photocatalytic reaction conditions.

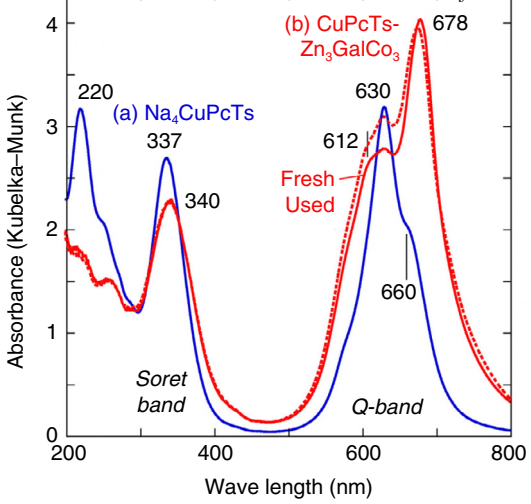

Figure 2

Diffuse-reflectance UV–visible absorption spectra for aqueous solution of a) $Na^+_4CuPcTs^{4-}$ (6.0 μmol L^{-1}) and b) CuPcTs-$Zn_3Ga|CO_3$. Solid line: fresh sample and dotted line: sample used after the photocatalytic test for 5 h.

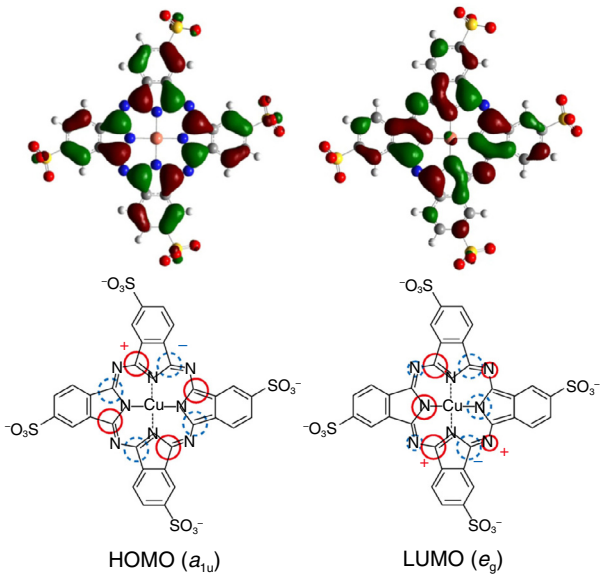

Figure 3

HOMO and LUMO for $Na^+_4CuPcTs^{4-}$ calculated using Gaussian 09.

Ag-$Zn_3Ga|CO_3$ and Au-$Zn_3Ga|CO_3$ exhibited a major absorption peak at 411 and 555 nm, respectively (not shown). These peaks are ascribed to Surface Plasmonic Resonance (SPR) of Ag and Au metallic nanoparticles.

The XANES spectra for $Na^{+}_{4}CuPcTs^{4-}$ and CuPcTs-$Zn_3Ga|CO_3$ are shown in Figure 4. The whole spectrum pattern changed negligibly by the dispersion of $CuPcTs^{4-}$ over the $Zn_3Ga|CO_3$ surface as compared with $Na^{+}_{4}CuPcTs^{4-}$ crystallines, suggesting that the framework structure of $CuPcTs^{4-}$ was retained upon the dispersion over the $Zn_3Ga|CO_3$ surface. In contrast, a sharp shoulder peak at 8 988 eV became relatively weaker upon the dispersion over the LDH surface. This may be related to the perturbation of LUMO by the interaction with the LDH surface based on UV–visible spectrum change (Fig. 2).

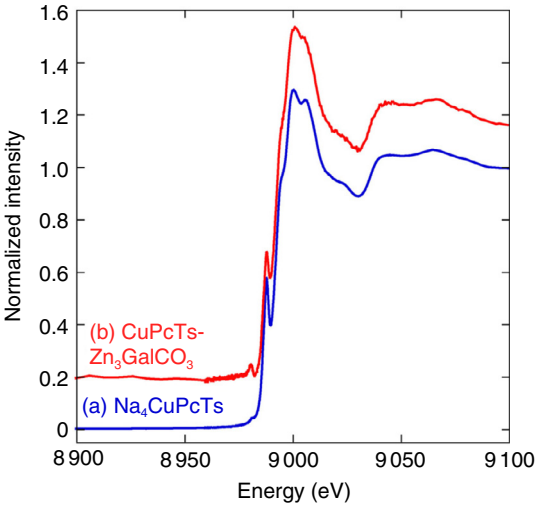

Figure 4

Normalized Cu K-edge XANES spectra for a) $Na^{+}_{4}CuPcTs^{4-}$ diluted by boron nitride and b) CuPcTs-$Zn_3Ga|CO_3$.

The 1s-3d electronic transition peak appeared at 8 982 eV for both $Na^{+}_{4}CuPcTs^{4-}$ and CuPcTs-$Zn_3Ga|CO_3$ (Fig. 5-I). The transition is allowed for the Cu^{II} state of the $3d^9$ configuration, whereas the peak disappeared for the Cu^{I} state of the $3d^{10}$ configuration (Morikawa *et al.*, 2014a). Utilizing this difference, the reduction of Cu^{II} sites in $Na^{+}_{4}CuPcTs^{4-}$ and CuPcTs-$Zn_3Ga|CO_3$ was monitored irradiated by UV–visible light.

The Cu amount in $Na^{+}_{4}CuPcTs^{4-}$ charged was 118 μmol. The decreasing rate of the 1s-3d peak irradiated by UV–visible light for 64 min was 18.0% h^{-1} or 21.2 μmol h^{-1}. In contrast, the Cu amount in CuPcTs-$Zn_3Ga|CO_3$ charged was 13.5 μmol. The decreasing rate of the 1s-3d peak irradiated by UV–visible light for 180 min was 20.2% h^{-1} or 2.72 μmol h^{-1} (Fig. 5-II). The photoreduction to the Cu(I) state was slightly faster for CuPcTs-$Zn_3Ga|CO_3$ than for $Na^{+}_{4}CuPcTs^{4-}$; however, exact comparison of the diffusion rates of photogenerated electrons to the Cu(II) site (Morikawa *et al.*, 2014a) was difficult in this case

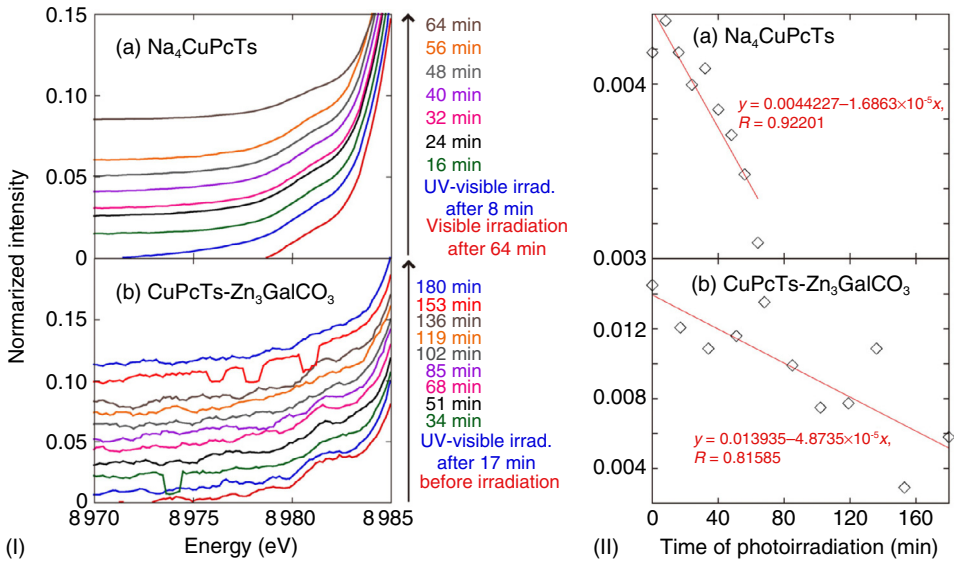

Figure 5

I) Expanded view of the 1s-3d pre-edge peak region of normalized Cu K-edge XANES spectra of a) $Na^{+}_{4}CuPcTs^{4-}$ under vacuum and b) CuPcTs-$Zn_3Ga|CO_3$ under CO_2 (2.3 kPa) + H_2 (21.7 kPa) and UV–visible light irradiation. II) Time course of the 1s-3d peak intensity for the two samples. The amount of $Na^{+}_{4}CuPcTs^{4-}$ and CuPcTs-$Zn_3Ga|CO_3$ charged in the photoreaction cell was 116 and 401 mg, respectively.

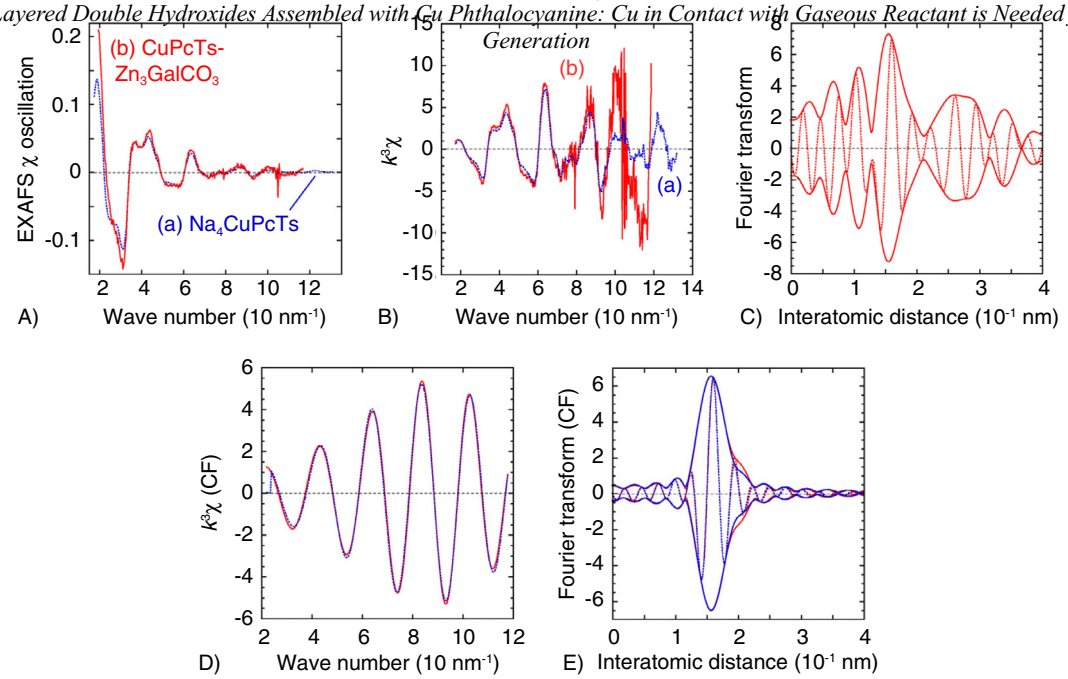

Figure 6

A) Cu K-edge EXAFS χ oscillation and B) k^3-weighted EXAFS χ oscillation for $Na^+_4CuPcTs^{4-}$ diluted by boron nitride (a) and CuPcTs-$Zn_3Ga|CO_3$ (b), C) its associated Fourier transform, and D, E) best-fit results in *k*-space D) and *R*-space E) for CuPcTs-$Zn_3Ga|CO_3$. Solid line: magnitude and dotted line: imaginary part C, E). Red (thick) line: experimental and blue (thin) line: fit D, E).

due to the difference in the shape and light absorbance of the samples: dense crystallines of $Na^+_4CuPcTs^{4-}$ *versus* fine powder of CuPcTs-$Zn_3Ga|CO_3$. At least, as the UV–visible light absorbance was apparently higher for $Na^+_4CuPcTs^{4-}$, the possibility of faster electron accumulation for CuPcTs-$Zn_3Ga|CO_3$ than $Na^+_4CuPcTs^{4-}$ is high due to the injection of excited electrons in $Zn_3Ga|CO_3$ irradiated by UV light into $CuPcTs^{4-}$ at the surface.

The EXAFS χ oscillation changed negligibly when $Na^+_4CuPcTs^{4-}$ was dispersed over the $Zn_3Ga|CO_3$ surface (Fig. 6A). This fact supported the retention of the $CuPcTs^{4-}$ framework over that of the $Zn_3Ga|CO_3$ suggested by XANES. The curve-fit results for the Cu–N interatomic pair provided a distance of 0.198 nm (fit error ±0.011 nm) with a *N* value of 3.3 (fit error ±1.3) (Fig. 6D, E).

2.2 Photocatalytic Tests under $CO_2 + H_2$

In the photocatalytic reaction tests under $CO_2 + H_2$ irradiated by UV–visible light, $Zn_3Ga|CO_3$ produced CO and methanol (Tab. 2A, entry a). Using $Zn_{1.5}Cu_{1.5}Ga|CO_3$, the methanol formation rate increased by a factor of 3.3 (Tab. 2A entry g). $Zn_3Al|CO_3$ was more active than $Zn_3Ga|CO_3$, but the major product was CO (entry h). When $Zn_{1.5}Cu_{1.5}Al|CO_3$ was compared with $Zn_3Al|CO_3$, the methanol formation rate was promoted by a factor of 3.3 (Tab. 2b entry i) similarly to the Cu substitution into $Zn_3Ga|CO_3$. The methanol formation rate using $Zn_3Ga|Cu(OH)_4$ was enhanced by a factor of 5.9 compared with $Zn_3Ga|CO_3$ (Tab.2A entries a, j). The methanol selectivity was nearly the same as that obtained with $Zn_{1.5}Cu_{1.5}Ga|CO_3$ (71-68 mol%). Using $Zn_{1.5}Cu_{1.5}Ga|Cu(OH)_4$, the methanol formation rate and selectivity were further improved to 0.49 μmol h^{-1} $g_{cat}{}^{-1}$ and 88 mol% (Tab. 2A entry k).

The results in Table 2 were independently reported in this study and references (Ahmed *et al*., 2011, 2012; Kawamura *et al*., 2015). However, the rates and selectivity are comparable because common reaction apparatus connected to common online GC were used in these studies. The reproducibility of rates was checked for $Zn_3Ga|CO_3$ in this study and references (Ahmed *et al*., 2011, 2012; Kawamura *et al*., 2015), and the variation of formation rates of methanol and CO was always within 5%.

Furthermore, we reported control reaction tests in darkness, in the absence of a photocatalyst, and in the absence of CO_2. No products were found in these control tests except

TABLE 2
Photocatalytic rates of CO_2 reduction with H_2 using LDH[a]

Entry	Photocatalyst	Formation rate ($nmol^{-1}g_{cat}$)			Selectivity to CH_3OH (mol%)	Reference
		CH_3OH	CO	Σ		
A) Irradiated by UV–visible light						
a	$Zn_3Ga\|CO_3$	51	80	130	39	Ahmed *et al.* (2011)
b	CuPcTs-$Zn_3Ga\|CO_3$	96	106	202	48	This work
b'	CuPcTs & $Zn_3Ga\|CO_3$[b]	28	41	69	41	This work
c	Zn_3Ga|CuPcTs	<4	69	69	<5	This work
d	$Na_4CuPcTs^{4-}$	<4	38	38	<9.5	This work
e	Ag–$Zn_3Ga\|CO_3$	118	102	220	54	Kawamura *et al.* (2015)
f	Au–$Zn_3Ga\|CO_3$[c]	30	201	231	13	Kawamura *et al.* (2015)
g	$Zn_{1.5}Cu_{1.5}Ga\|CO_3$	170	79	250	68	Ahmed *et al.* (2011)
h	$Zn_3Al\|CO_3$	39	620	660	5.9	Ahmed *et al.* (2011)
i	$Zn_{1.5}Cu_{1.5}Al\|CO_3$	130	370	500	26	Ahmed *et al.* (2011)
j	$Zn_3Ga\|Cu(OH)_4$	300	130	430	71	Ahmed *et al.* (2012)
k	$Zn_{1.5}Cu_{1.5}Ga\|Cu(OH)_4$	490	70	560	88	Ahmed *et al.* (2012)
B) Irradiated by visible light ($\lambda > 420$ nm)						
a	$Zn_3Ga\|CO_3$	<4	<8	<12	<33	Ahmed *et al.* (2011)
b	CuPcTs-$Zn_3Ga\|CO_3$	75	74	148	51	This work
c	Zn_3Ga|CuPcTs	<4	33	33	<11	This work
d	Ag–$Zn_3Ga\|CO_3$	36	88	124	29	Kawamura *et al.* (2015)
e	Au–$Zn_3Ga\|CO_3$[c]	<4	<8	<12	<33	Kawamura *et al.* (2015)

[a] In CO_2 (2.3 kPa) + H_2 (21.7 kPa). The catalyst amount was 100 mg.
[b] Physical mixture with the weight ratio of 3:97.
[c] Preheated at 373 K for 30 min.

for water from the interlayer space of the LDH. When the reactant was switched from CO_2 to CO_2 + H_2, methanol and CO began to evolve using $Zn_{1.5}Cu_{1.5}Ga|CO_3$ (Ahmed *et al.*, 2011). When the $Zn_{1.5}Cu_{1.5}Ga|CO_3$ and $Zn_{1.5}Cu_{1.5}Ga|Cu(OH)_4$ photocatalysts were recycled four times (in total 20 h of reaction), the methanol and CO formation continued and the selectivity was kept at 68-57 mol% and 76-84 mol%, respectively (Ahmed *et al.*, 2011, 2013).

The addition of $CuPcTs^{4-}$ to $Zn_3Ga|CO_3$ improved the total (methanol and CO) formation rates by a factor of 1.6 and the methanol selectivity increased to 48 mol% (Tab. 2A entry b; Fig. 7a-line). The formation of CO and methanol continued for more than 5 h, demonstrating the stability of dispersed $CuPcTs^{4-}$ over the LDH irradiated by UV–visible light under CO_2 + H_2. In contrast, the performance of Zn_3Ga|CuPcTs was lower than that of $Zn_3Ga|CO_3$ (Tab. 2A entry c and Fig. 7b-line). It should be noted that unsupported $Na^+{}_4CuPcTs^{4-}$ generated CO at a rate of 48% of that using $Zn_3Ga|CO_3$ (Tab. 2A entry d).

In a control kinetic test using the physical mixture of 3.0 wt% of $Na^+{}_4CuPcTs^{4-}$ and 97 wt% of $Zn_3Ga|CO_3$ LDH prepared by mixing using a mortar and pestle for 30 min, the formation rates of CO and methanol were 41 and 28 μmol h^{-1} $g_{cat}{}^{-1}$, respectively (Tab. 2A entry b), suggesting the importance of close contact of $CuPcTs^{4-}$ with the LDH surface for the CO_2 photoconversion using CuPcTs-$Zn_3Ga|CO_3$ (Fig. 7a-line).

The addition of Ag to $Zn_3Ga|CO_3$ similarly affected the addition of $CuPcTs^{4-}$. Total formation rates increased by a factor of 1.7 compared with $Zn_3Ga|CO_3$ and methanol

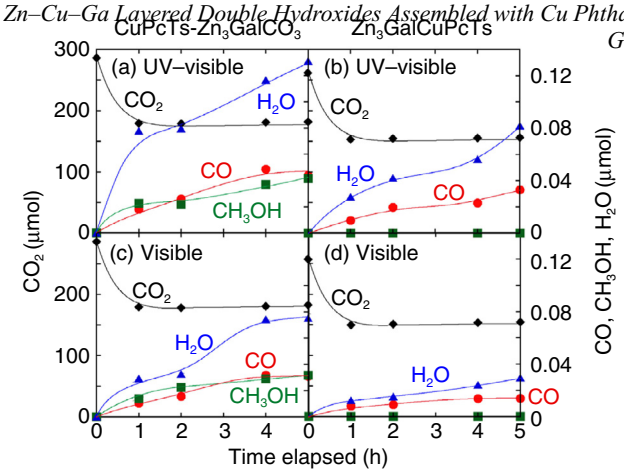

Figure 7

Time course of photocatalytic tests under CO_2 (2.3 kPa) and H_2 (21.7 kPa) using UV–visible light and a) CuPcTs-$Zn_3Ga|CO_3$ and b) $Zn_3Ga|$CuPcTs; and using visible light ($\lambda > 420$ nm) and c) CuPcTs-$Zn_3Ga|CO_3$ and d) $Zn_3Ga|$CuPcTs. CO_2 (◆; diamond), H_2O (▲; triangle), CH_3OH (■; square), and CO (●; circle).

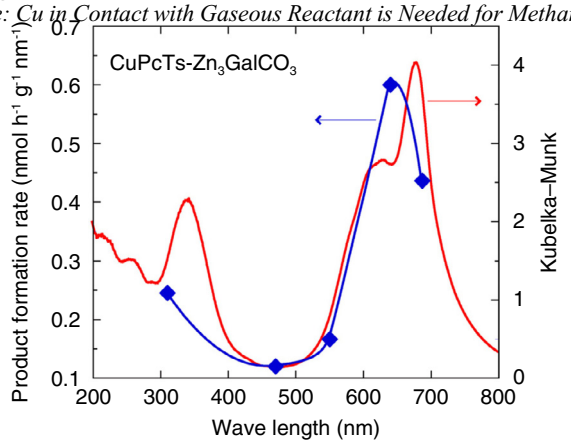

Figure 8

In-profile spectrum for CuPcTs-$Zn_3Ga|CO_3$.

selectivity of 54 mol% (Tab. 2A entry e). The addition of Au to $Zn_3Ga|CO_3$ promoted the total formation rates by a factor of 1.8, but the methanol selectivity became only 13 mol% (Tab. 2A entry f).

Next, photocatalytic reduction tests of CO_2 by H_2 were conducted irradiated by visible light ($\lambda > 420$ nm). Although the $Zn_3Ga|CO_3$ LDH showed poor photoactivity irradiated by visible light (Tab. 2B entry a), the total formation rate using CuPcTs-$Zn_3Ga|CO_3$ irradiated by visible light was 73% of that irradiated by UV–visible light (Tab. 2B entry b). The methanol selectivity was maintained at 48-51 mol% (Fig. 7 c-line). Again, under the condition of visible light irradiation, the formation of CO and methanol continued for more than 5 h, demonstrating the stability of dispersed $CuPcTs^{4-}$ over the LDH under $CO_2 + H_2$.

The total formation rate using Ag-$Zn_3Ga|CO_3$ irradiated by visible light was 56% of that irradiated by UV–visible light (Tab. 2A entry c, Tab. 2B entry d). The selectivity to methanol decreased from 54 mol% (irradiated by UV–visible light) to 29 mol% (irradiated by visible light). Thus, Ag was less effective than $CuPcTs^{4-}$ as a promoter under the condition of visible light irradiation. In comparison with the addition of $CuPcTs^{4-}$ and Ag, Au-$Zn_3Ga|CO_3$ did not exhibit photocatalytic activity above the detection limit of GC irradiated under visible light (Tab. 2B, entry e).

The promotion effect of $CuPcTs^{4-}$ to $Zn_3Ga|CO_3$ was further investigated by plotting the in-profile (action) spectrum of total formation rates (methanol and CO) based on the photocatalytic tests irradiated by the light of wavelengths progressively greater than 420, 520, 580, 620, 660 and 715 nm using sharp cut filters (Fig. 8). The in-profile spectrum and UV–visible absorption spectrum coincided well in the wavelength ranges 310 and 688 nm, demonstrating that the visible light absorption by $CuPcTs^{4-}$ dispersed over $Zn_3Ga|CO_3$ (Fig. 2b-line) led to electron excitation and then the reduction of CO_2.

3 DISCUSSION

$Zn_3Ga|CO_3$ exhibited photocatalytic reduction of CO_2 by H_2 and UV–visible light at a total formation rate (methanol and CO) of 130 nmol h^{-1} $g_{cat}{}^{-1}$ (Tab. 2A, entry a). When the amount of photocatalyst varied between 25 and 100 mg, the formation rate (the unit: mol h^{-1}) was essentially proportional to the amount (Ahmed *et al.*, 2011; Yoshida *et al.*, 2012).

Copper ions were doped as a part of M^{II} cations in the cationic layer $[M^{II}{}_{1-x}M^{III}{}_x(OH)_2]^{x+}$ of LDH and/or $Cu(OH)_4{}^{2-}$ anions between the cationic layers. Both inlayer and interlayer Cu sites were effective for photocatalytic reduction of CO_2 (Ahmed *et al.*, 2011, 2012). As a result, the total formation rate using $Zn_{1.5}Cu_{1.5}Ga|Cu(OH)_4$ was 560 nmol h^{-1} $g_{cat}{}^{-1}$ (Tab. 2A, entry k). Copper sites were primarily active for photocatalytic reduction of CO_2 by H_2.

The drawback of LDH comprising Cu was the limitation of the wavelength for excitation light. The estimated E_g values for the LDH used in this study were 5.6-3.0 eV (Tab. 1), indicating that only UV light was effective for CO_2 photoreduction using LDH comprising Cu. To overcome this drawback, $CuPcTs^{4-}$, Ag or Au was doped to $Zn_3Ga|CO_3$.

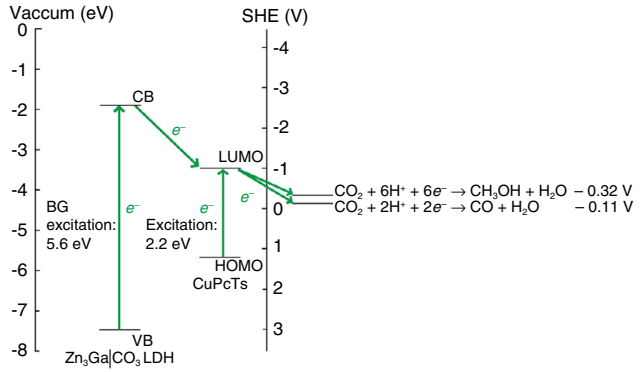

Figure 9

The energy diagram and proposed electron flows in CuPcTs-$Zn_3Ga|CO_3$ during photocatalytic reduction of CO_2.

$CuPcTs^{4-}$, Ag or Au in CuPcTs-$Zn_3Ga|CO_3$, Ag-$Zn_3Ga|CO_3$ and Au-$Zn_3Ga|CO_3$ photocatalysts were effective at boosting methanol and CO formation rates by a factor of 1.6-1.8 compared with $Zn_3Ga|CO_3$, both irradiated by UV–visible light (Tab. 2A). The interlayer distance of the LDH changed negligibly for these photocatalysts (Fig. 1), demonstrating $CuPcTs^{4-}$, Ag and Au were over the exterior surface of the LDH rather than the interlayer space (Kawamura *et al.*, 2015). Under UV–visible light, band-gap excitation of the LDH occurred by UV light (Tab. 1), while HOMO–LUMO excitation (2.2 eV, Fig. 9; Giraudeau *et al.*, 1980; Shang *et al.*, 2011) of $CuPcTs^{4-}$ and SPR of Ag and Au nanoparticles occurred by visible light.

The photocatalytic effects of UV and visible light were clarified by the photocatalytic tests irradiated by visible light only (Tab. 2B), and also the in-profile spectrum of CO_2 photoreduction (Fig. 8). The formation rates of methanol and CO irradiated by visible light were 73-56% of those irradiated by UV–visible light using CuPcTs-$Zn_3Ga|CO_3$ and Ag-$Zn_3Ga|CO_3$, whereas Au-$Zn_3Ga|CO_3$ did not exhibit photocatalytic activity above the detection limit of GC under the irradiation of visible light. Thus, $CuPcTs^{4-}$ was the best promoter for the LDH irradiated by visible light. The stability of $CuPcTs^{4-}$ during photocatalytic tests was demonstrated (Fig. 2, 7a-c-line). Because the E_g value for $Zn_3Ga|CO_3$ was 5.6 eV (Tab. 1), the LDH did not participate in the catalysis under visible light but just dispersed $CuPcTs^{4-}$ molecules on the external surface.

The energy diagram and proposed electron flow during CO_2 photoreduction using CuPcTs-$Zn_3Ga|CO_3$ are depicted in Figure 9. As the HOMO–LUMO gap positions between Valence Bands (VB) and Conduction Bands (CB) of $Zn_3Ga|CO_3$, band-gap excited electrons at CB and resultant holes at VB transfer to LUMO and HOMO of $CuPcTs^{4-}$, respectively, irradiated by UV light. In fact, photogenerated electrons diffused to the central Cu(II) site of $CuPcTs^{4-}$ at the rates of 2.7-21 μmol h^{-1} for $Na^+{}_4CuPcTs^{4-}$ and CuPcTs-$Zn_3Ga|CO$ (Fig. 5). $Na^+{}_4CuPcTs^{4-}$ was able to photocatalyze CO_2 to CO by H_2 (Tab. 2A, entry d). When CuPcTs-$Zn_3Ga|CO_3$ was irradiated by visible light only, the band-gap excitation (5.6 eV) of $Zn_3Ga|CO_3$ did not take place and only HOMO–LUMO excitation (2.2 eV) of $CuPcTs^{4-}$ was possible. The decrease in the formation rates of methanol and CO under visible light to 73% of those under UV–visible light (Tab. 2) can be explained by the decrease in the electron and hole supply from $Zn_3Ga|CO_3$ to $CuPcTs^{4-}$.

The LUMO of $CuPcTs^{4-}$ does not exactly populate Cu sites but N atoms neighboring Cu sites (Fig. 3). Thus, the electrons excited to the CB of the LDH would transfer to LUMO (and/or an unoccupied level near LUMO) of $CuPcTs^{4-}$. The energy level diagram of the LDH and $CuPcTs^{4-}$ supported this hypothesis (Fig. 9).

The HOMO dominantly distribute on C atoms of pyrrole rings, while the LUMO dominantly distribute on both C and N atoms of pyrrole rings for $CuPcTs^{4-}$ (Rauf *et al.*, 2012). The N atoms of pyrrole are bonded to central Cu^{2+} ions and thus able to transfer the photo-excited electrons to Cu^{2+} (Fig. 3). CO_2 would be progressively reduced by the reduced Cu^+ in a similar way to that by inlayer and interlayer Cu sites (Morikawa *et al.*, 2014a; Ahmed *et al.*, 2011, 2012). On the other hand, H_2 would donate an electron to the position around HOMO (Fig. 3) to form H^+. The proton combines the electron and CO_2 at the Cu site and finally transforms into CO and methanol.

The SPR effect of Ag nanoparticles was already discussed in reference (Kawamura *et al.*, 2015). In contrast, SPR of Au was not effective for the photoreduction of CO_2 due to the greater work function of Au (5.31-5.47 eV) as compared with that of Ag (4.52-4.74 eV). Irradiated by UV–visible light, the Au surface played the role of an electron trap from $Zn_3Ga|CO_3$.

LDH compounds especially comprising Cu and Ga selectively photoproduced methanol from $CO_2 + H_2$ (68-88 mol%, Tab. 1). A reaction mechanism *via* hydrogen carbonate bound to Cu was proposed based on FTIR and XAFS (Ahmed *et al.*, 2011; Morikawa *et al.*, 2014a). These LDH photocatalysts would be combined with a photooxidation catalyst, *e.g.* WO_3, to produce methanol from $CO_2 + H_2O$ (Morikawa *et al.*, 2014b).

CONCLUSIONS

LDH comprising Zn and Al or Ga photoreduced CO_2 to CO and methanol by H_2 and the irradiation of UV–visible light.

When Cu ions were doped as cations in the cationic layer and/or as interlayer anions, the CO_2 photoreduction rates increased to as high as 560 nmol h^{-1} $g_{cat}{}^{-1}$ ($Zn_{1.5}Cu_{1.5}Ga|Cu(OH)_4$ photocatalyst). Due to the wide band-gap nature of these LDH, UV light was effective for CO_2 photoreduction. The doping of $CuPcTs^{4-}$ and Ag to the $Zn_3Ga|CO_3$ LDH boosted CO_2 photoreduction by a factor of 1.6-1.8 by H_2 and the irradiation of UV–visible light. $CuPcTs^{4-}$ was especially effective doped to the LDH for CO_2 photoreduction irradiated by visible light only. The LUMO of $CuPcTs^{4-}$ was distributed on N atoms of pyrrole rings bound to central Cu^{2+} ions. The photo-excited electrons diffused to central Cu^{2+} would progressively reduce CO_2 finally to CO and methanol in a similar way to the inlayer and interlayer Cu sites in the LDH in this study.

ACKNOWLEDGMENTS

The authors are grateful for the financial support from the Grant-in-Aid for Scientific Research C (26410204, 22550117) from the Japan Society for the Promotion of Science, *Asahi Grass* Foundation, Promotion Section of Technology Innovation, *Daikin Industries*, and from the Romanian National Authority for Scientific Research (PN-II-IDEI-PCE-75/2013). X-ray absorption experiments were conducted under the approval of the Photon Factory Proposal Review Committee (2011G033, 2009G552, 2007G576) and Grant of the Priority Program for Disaster-Affected Quantum Beam Facilities (2011A1977, SPring-8 & KEK).

REFERENCES

Abellán G., Busolo F., Coronado E., Martí-Gastaldo C., Ribera A. (2012) Hybrid Magnetic Multilayers by Intercalation of Cu(II) Phthalocyanine in LDH Hosts, *J. Phys. Chem. C* **116**, 29, 15756-15764.

Ahmed N., Morikawa M., Izumi Y. (2013) Photocatalytic Conversion of Carbon Dioxide into Fuels Using Layered Double Hydroxides Coupled with Hydrogen or Water, in *New and Future Developments in Catalysis: Activation of Carbon Dioxide*, Suib S.L. (ed.), Elsevier, pp. 589-602.

Ahmed N., Morikawa M., Izumi Y. (2012) Photocatalytic conversion of carbon dioxide into methanol using optimized layered double hydroxide catalysts, *Catal. Today* **185**, 263-269.

Ahmed N., Shibata Y., Taniguchi T., Izumi Y. (2011) Photocatalytic conversion of carbon dioxide into methanol using zinc-copper-M (III) (M = aluminum, gallium) layered double hydroxides, *J. Catal.* **279**, 123-135.

Bearden J.A. (1967) X-Ray Wavelengths, *Rev. Mod. Phys.* **39**, 1, 78-124.

Carrera F., Marcos E.S., Merkling P.J., Chaboy J., Muñoz-Páez A. (2004) Nature of Metal Binding Sites in Cu(II) Complexes with Histidine and Related N-Coordinating Ligands, As Studied by EXAFS, *Inorg. Chem.* **43**, 21, 6674-6683.

Carja G., Birsanu M., Okada K., García H. (2013) Composite plasmonic gold/layered double hydroxides and derived mixed oxides as novel photocatalysts for hydrogen generation under solar irradiation, *J. Mater. Chem. A* **1**32, 9092-9098.

Cavani F., Trifirò F., Vaccari A. (1991) Hydrotalcite-type anionic clays: preparation, properties and applications, *Catal. Today* **11**, 173-301.

Costentin C., Robert M., Savéant J.M. (2013) Catalysis of the electrochemical reduction of carbon dioxide, *Chem. Soc. Rev.* **42**, 6, 2423-2436.

Corma A., García H. (2013) Photocatalytic reduction of CO_2 for fuel production: Possibilities and challenges, *J. Catal.* **308**, 168-175.

Fan G., Li F., Evans D.G., Duan X. (2014) Catalytic applications of layered double hydroxides: recent advances and perspective, *Chem. Soc. Rev.* **43**, 20, 7040-7066.

Genevese C., Ampelli C., Parathoner S., Centi G. (2013) Electrocatalytic conversion of CO_2 to liquid fuels using nanocarbon-based electrodes, *J. Energy Chem.* **22**, 2, 202-213.

Giraudeau A., Fan F.F., Bard A.J. (1980) Semiconductor Electrodes. 30. Spectral Sensitization of the Smiconductors *n*-TiO_2 and *n*-WO_3 with Metal Phthalocyanines, *J. Am. Chem. Soc.* **102**, 16, 5137-5142.

Habisreutinger S.N., Schmidt-Mende L., Stolarczyk J.K. (2013) Photocatalytic Reduciton of CO_2 on TiO_2 and Other Semiconductors, *Angew. Chem. Int. Ed.* **52**, 29, 7372-7408.

Indrakanti V.P., Kubicki J.D., Schobert H.H. (2009) Photoinduced activation of CO_2 on Ti-based heterogeneous catalysts: Current state, chemical physics-based insights and outlook, *Energy Environ. Sci.* **2**, 7, 745-758.

Izumi Y. (2013) Recent advances in the photocatalytic conversion of carbon dioxide to fuels with water and/or hydrogen using solar energy and beyond, *Coord. Chem. Rev.* **257**, 171-186.

Izumi Y., Itoi T., Peng S., Oka K., Shibata Y. (2009) Site Structure and Photocatalytic Role of Sulfur or Nitrogen-Doped Titanium Oxide with Uniform Mesopores under Visible Light, *J. Phys. Chem. C* **113**, 16, 6706-6718.

Izumi Y., Konishi K., Obaid D., Miyajima T., Yoshitake H. (2007) X-ray Absorption Fine Structure Combined with X-ray Fluorescence Spectroscopy. Monitoring of Vanadium Sites in Mesoporous Titania, Excited under Visible Light by Selective Detection of Vanadium $K\beta_{5,2}$ Fluorescence, *Anal. Chem.* **79**, 18, 6933-6940.

Izumi Y., Kiyotaki F., Yagi N., Vlaicu A.M., Nisawa A., Fukushima S., Yoshitake H., Iwasawa Y. (2005) X-ray Absorption Fine Structure Combined with X-ray Fluorescence Spectrometry. Part 15. Monitoring of Vanadium Site Transformations on Titania and in Mesoporous Titania by Selective Detection of the Vanadium $K\alpha_1$ Fluorescence, *J. Phys. Chem.* **109**, 31, 14884-14891.

Kawamura S., Cornelia P.M., Yoshida Y., Izumi Y., Carja G. (2015) Tailoring assemblies of plasmonic silver/gold and zinc-gallium layered double hydroxides for photocatalytic conversion of carbon dioxide using UV-visible light, DOI: 10.1016/j.apcata.2014.12.042.

Kubacka A., Fernández-García M., Colón G. (2012) Advanced Nanoarchitectures for Solar Photocatalytic Applications, *Chem. Rev.* **112**, 3, 1555-1614.

Lewis N.S., Nocera D.G. (2006) Powering the planet: Chemical challenges in solar energy utilization, *Proc. Natl. Acad. Sci. U. S. A.* **103**, 43, 15729-15735.

Li C., Wei M., Evans D.G., Duan X. (2014) Layered Double Hydroxide-based Nanomaterials as Highly Efficient Catalysts and Adsorbents, *Small* **10**, 22, 4469-4486.

Lv H., Geletii Y.V., Zhao C., Vickers J.W., Zhu G., Luo Z., Song J., Lian T., Musaev D.G., Hill C.L. (2012) Polyoxometalate water oxidation catalysts and the production of green fuel, *Chem. Soc. Rev.* **41**, 22, 7572-7589.

Marom N., Hod O., Scuseria G.E., Kronik L. (2008) Electronic structure of copper phthalocyanine: A comparative density functional theory study, *J. Chem. Phys.* **128**, 16, 164107.

Morikawa M., Ahmed N., Yoshida Y., Izumi Y. (2014a) Photoconversion of carbon dioxide in zinc-copper-gallium layered double hydroxides: The kinetics to hydrogen carbonate and further to CO/methanol, *Appl. Catal. B* **144**, 561-569.

Morikawa M., Ogura Y., Ahmed N., Kawamura S., Mikami G., Okamoto S., Izumi Y. (2014b) Photocatalytic conversion of carbon dioxide into methanol in reverse fuel cells with tungsten oxide and layered double hydroxide photocatalysts for solar fuel generation, *Catal. Sci. Technol.* **4**, 6, 1644-1651.

Parida K.M., Baliarsingh N., Patra B.S., Das J. (2007) Copperphthalocyanine immobilized Zn/Al LDH as photocatalyst under solar radiation for decolorization of methylene blue, *J. Mol. Catal. A.* **267**, 202-208.

Rauf M.A., Hisaindee S., Graham J.P., Nawaz M. (2012) Solvent effects on the absorption and fluorescence spectra of Cu(II)-phthalocyanine and DFT calculations, *J. Mol. Liquids* **168**, 102-109.

Roy S.C., Varghese O.K., Paulose M., Grimes C.A. (2010) Toward Solar Fuels: Photocatalytic Conversion of Carbon Dioxide to Hydrocarbons, *ACS Nano* **4**, 3, 1259-1278.

Shang J., Zhao F., Zhu T., Li J. (2011) Photocatalytic degradation of rhodamine B by dye–sensitized TiO_2 under visible-light irradiation, *Sci. China Chem.* **54**, 1, 167-172.

Sideris P.J., Nielsen U.G., Gan Z., Grey C.P. (2008) Mg/Al Ordering in Layered Double Hydroxides Revealed by Multinuclear NMR Spectroscopy, *Science* **321**, 5885, 113-117.

Vaarkamp M., Linders H., Koningsberger D. (2006) *XDAP version 2.2.7*, XAFS Services International, Woudenberg, The Netherlands.

Wooten F. (1972) *Optical Properties of Solids*, Academic Press, New York, USA, p. 142.

Yoshida Y., Mitani Y., Itoi T., Izumi Y. (2012) Preferential oxidation of carbon monoxide in hydrogen using zinc oxide photocatalysts promoted and tuned by adsorbed copper ions, *J. Catal.* **287**, 190-202.

Zümreoglu-Karan B., Ay A.N. (2012) Layered double hydroxide–multifunctional nanomaterials, *Chem. Papers* **66**, 1, 1-10.

Manuscript submitted in October 2014
Manuscript accepted in May 2015
Published online in September 2015

Cite this article as: S. Kawamura, N. Ahmed, G. Carja and Y. Izumi (2015). Photocatalytic Conversion of Carbon Dioxide Using Zn–Cu–Ga Layered Double Hydroxides Assembled with Cu Phthalocyanine: Cu in Contact with Gaseous Reactant is Needed for Methanol Generation, *Oil Gas Sci. Technol* **70**, 5, 841-852.